Check for updates

The effects of alkylthio chains on the properties of symmetric liquid crystal dimers†

Ewan Cruickshank, [ID] *[a] Grant J. Strachan, [ID] [a] Magdalena M. Majewska, [ID] [b] Damian Pociecha, [ID] [b] Ewa Gorecka, [ID] [b] John M. D. Storey [ID] [a] and Corrie T. Imrie [ID] [a]

The synthesis and characterisation of four series of symmetric liquid crystal dimers containing either alkylthio or alkyloxy terminal chains are reported. The (*E,E*)-[pentane-1,5-diylbis(oxy-4,1-phenylene)]bis{*N*-[4-(alkyloxy)phenyl]methanimine}s, *m*O.O5O.O*m* and (*E,E*)-[hexane-1,6-diylbis(oxy-4,1-phenylene)]bis{*N*-[4-(alkyloxy)phenyl]methanimine}s, *m*O.O6O.O*m* series are nematogenic when the terminal chains are short whereas the higher homologues show the smectic A phase. The *m*O.O6O.O*m* series shows higher clearing temperatures regardless of the terminal chain length. The (*E,E*)-[pentane-1,5-diylbis(oxy-4,1-phenylene)]bis{*N*-[(alkylthio)phenyl]methanimine}s, *m*S.O5O.S*m* series is solely nematogenic, and does not show liquid crystallinity when *m* ≥ 5. The (*E,E*)-[hexane-1,6-diylbis(oxy-4,1-phenylene)]bis{*N*-[(alkylthio)phenyl]methanimine}s, *m*S.O6O.S*m* series, however, shows mesogenic behavior over the entire series, with the smectic C phase only emerging when the terminal chain is long, *m* ≥ 8. In general, for a given spacer length, the dimers containing alkyloxy chains show the highest clearing temperatures and the alkylthio chains the lowest. For the shortest terminal chains, however, the nematic−isotropic transition temperatures of the alkylthio materials are higher than those containing the alkyl chain. This behaviour is rather general and discussed in terms of steric and electronic interactions.

[a] Department of Chemistry, University of Aberdeen, Old Aberdeen, AB24 3UE, UK.
E-mail: ewan.cruickshank2@abdn.ac.uk
[b] Faculty of Chemistry, University of Warsaw, ul. Zwirki i Wigury 101, 02-089,
Warsaw, Poland
† Electronic supplementary information (ESI) available. See DOI: **https://doi.org/10.1039/d2nj06252f**

Introduction

In the design of organic molecules, sulfur can be interchanged with oxygen and during the 1960s and 1970s, in particular, saw use in liquid crystals.[1–4] There has been a recent resurgence of interest in sulfur containing mesogens and the inclusion of sulfur has been achieved using, for example, terminal alkylthio chains,[5–14] thiophene moieties,[15–18] thiocyanate terminal groups,[19,20] and thioester linking groups.[21,22] The motivation for including sulfur in mesogenic materials is the increase in birefringence arising from the high polarisability of the sulfur atom.[7,9,10,23] Highly birefringent mesogenic materials are of significant technological interest in areas such as fast third-order non-linear switching,[21] liquid crystal displays,[24,25] liquid crystal lenses,[26–28] laser applications[29] and colour tunable plasmonic devices.[30,31] At a fundamental level, the inclusion of sulfur provides a demanding challenge to our understanding of structure–property relationships in low molar mass liquid crystals.[5,8,10,11,32,33]

Conventional low molar mass calamitic liquid crystalline materials consist of molecules that contain a single rod-like mesogenic unit, with one or two terminal alkyl chains attached. In essence the interactions between the semi-rigid mesogenic cores give rise to the liquid crystalline behaviour and the terminal chains lower the melting point. Liquid crystal dimers, however, are composed of molecules containing two rod-like mesogenic units connected by a flexible spacer[34,35] and have attracted considerable interest in recent years following the discovery of the twist-bend nematic[36–39] and twist-bend smectic phases.[40–42] The flexible spacer is normally an alkyl chain and largely controls the molecular shape. In essence, for an even-membered spacer, the mesogenic units are parallel and the dimer linear, whereas for an odd-membered spacer, the mesogenic units are inclined at some angle with respect to each other and so the dimer is bent. Liquid crystal dimers may be considered to have an inversion of the conventional low molar mass liquid crystal structure by having a highly flexible core.[43] Sulfur atoms have been incorporated into the spacer of liquid crystal dimers previously[44–46] and used as the link between the spacer and the mesogenic units.[47–56] The role of the terminal chains in liquid crystal dimers is to exert control, at least to some extent, over the melting point and phase behaviour. It was originally suggested that the inherent flexibility of liquid crystal dimers would inhibit the formation of smectic phases, This was
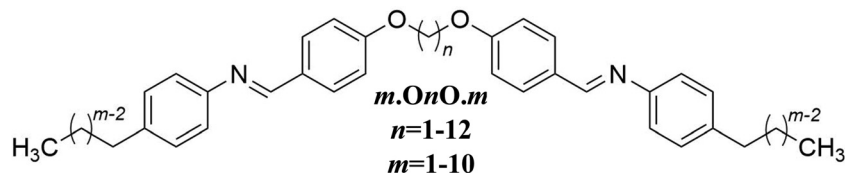
Fig. 1 The molecular structure of the *m*.O*n*O.*m* family of dimers.[57]

shown, however, not to be the case by Date *et al.*,[57] who reported extensive smectic polymorphism in the family of dimers referred to as *m*.O*n*O.*m* where *n* is the number of methylene units in the spacer and *m* the length of the terminal alkyl chains, see Fig. 1. In these materials, a simple relationship was established linking the observation of smectic phase behaviour to the values of *n* and *m*, specifically, smectic phases formed when $m > n/2$.

There have been very few reports describing liquid crystal dimers containing terminal alkylthio chains.[58–60] Here we explore how changing the nature of the links between the terminal chains and mesogenic units effects the phase behaviour of symmetric liquid crystal dimers with a particular focus on the thioether link. We report the synthesis and characterisation of the materials corresponding to the *m*.O*n*O.*m* family but containing thioether links, the *m*S.O*n*O.S*m* family, Fig. 2, and ether links the *m*O.O*n*O.O*m* family, Fig. 3. For both sets of materials, an even- and odd-membered spacer has been used and the terminal chain varied from 1 to 9 carbon atoms.

Experimental

Synthesis

The synthetic route used to prepare the *m*S.O*n*O.S*m* series is shown in Scheme 1 and for the *m*O.O*n*O.O*m* series in Scheme 2. A detailed description of the preparation of these series, including the structural characterisation data for all intermediates and final products, is provided in the ESI.†

Optical studies

Phase characterisation was performed by polarised light microscopy, using an Olympus BH2 microscope equipped with a Linkam TMS 92 hot stage. The untreated glass slides were 0.17 mm thickness. To obtain planarly aligned samples, polymer-treated glass cells with a thickness of 2.9–3.5 μm, purchased from INSTEC, were used.

Differential scanning calorimetry

The phase behaviour of the materials was studied by differential scanning calorimetry performed using a Mettler Toledo DSC1 or DSC3 differential scanning calorimeter equipped with TSO 801RO sample robots and calibrated using indium and zinc standards. Heating and cooling rates were 10 °C min⁻¹, with a 3 min isotherm between either heating or cooling, and all samples were measured under a nitrogen atmosphere. Transition temperatures and associated enthalpy changes were extracted from the heating traces unless otherwise noted.

Molecular modelling

The geometric parameters of the *m*O.O*n*O.O*m* and *m*S.O*n*O.S*m* series were obtained using quantum mechanical DFT calculations with Gaussian09 software.[61] Optimisation of the thioether-linked molecular structures was carried out at the B3LYP/6-311G(d,p) level of theory. Comparison of the results of optimisation of the methylene- and ether-linked materials at the B3LYP/6-311G(d,p) and the 6-31G(d) levels showed no discernible difference in the geometries found, and so optimisation of the methylene- and ether-linked materials was carried out at the B3LYP/6-31G(d) level. Visualisations of electronic surfaces were generated from the optimised geometries using the GaussView 5 software, and visualisations of the space-filling models were produced post-optimisation using the QuteMol package.[62]

X-Ray diffraction

The wide-angle X-ray diffraction (XRD) measurements were obtained with a Bruker D8 GADDS system (CuKα line, Goebel mirror, point beam collimator, Vantec2000 area detector). The small angle X-ray diffraction (SAXS) patterns for powder samples were obtained with a Bruker Nanostar system using CuKα radiation and patterns were collected with a Vantec2000 area detector. The temperature of the sample was controlled with precision of ±0.1 K. Samples were prepared as droplets on a heated surface.

Results and discussion

The transitional properties for the *m*O.O5O.O*m* series are listed in Table 1. The transition temperatures for *m* = 2 were found to be in good agreement with those reported elsewhere.[63] The homologues with a terminal alkoxy chain of $m \leq 4$ showed a

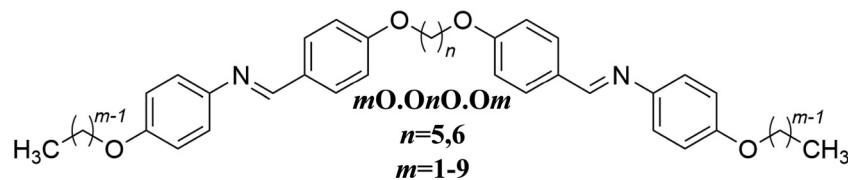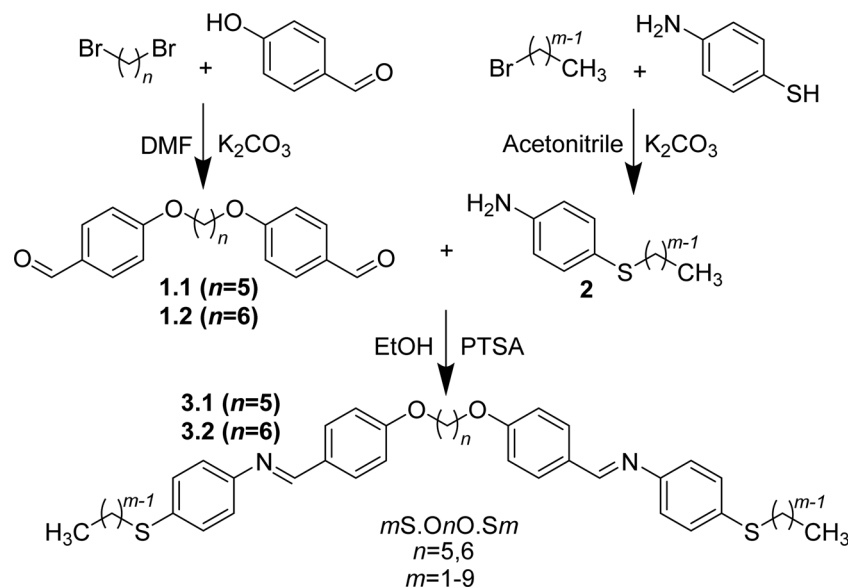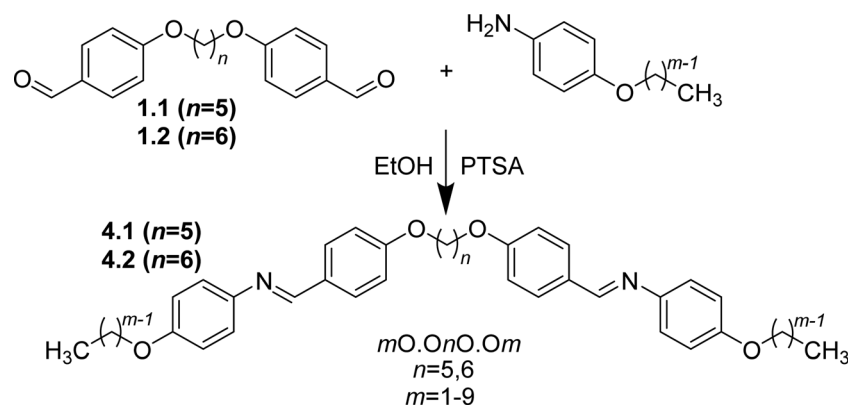Fig. 2 The molecular structure of the *m*S.O*n*O.S*m* family of dimers.

Fig. 3 The molecular structure of the mO.OnO.Om family of dimers.

Scheme 1 Synthesis of the mS.OnO.Sm series.

Scheme 2 Synthesis of the mO.OnO.Om series.

conventional nematic phase, N, which was assigned using the textures observed with polarised optical microscopy. Specifically, when sandwiched between two untreated glass slides, a characteristic schlieren texture was observed containing both two- and four-brush point defects, which flashed when subjected to mechanical stress, Fig. 4(a). These assignments are supported by the values of $\Delta S_{NI}/R$ which are typical for odd-membered dimers.[64,65] On cooling 5O.O5O.O5, there was a

cessation of the optical flickering associated with director fluctuations in the nematic phase and a focal conic fan texture developed which could be sheared to give homeotropic regions. These observations are consistent with the lower temperature phase being a uniaxial smectic A phase. For the homologues with $m \geq 6$, a focal conic fan texture formed directly from the isotropic phase and was observed in co-existence with homeotropic regions, Fig. 4(b), and this is assigned as a SmA–I
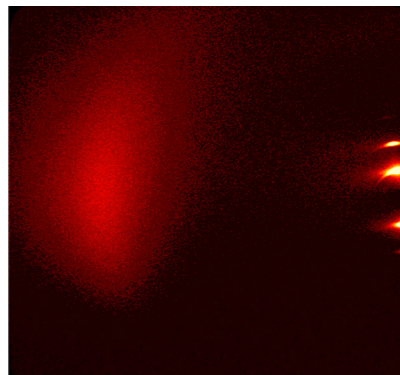
Table 1 Transition temperatures and associated scaled entropy changes for the mO.O5O.Om series

m	T_{Cr-}/°C	T_{SmAN}/°C	T_{NI}/°C T_{SmAI}*/°C	ΔS_{Cr-}/R	ΔS_{SmAN}/R	ΔS_{NI}/R ΔS_{SmAI}/R*
1	185	—	195	13.6	—	0.35
2	182	—	204	12.2	—	0.49
3	183	—	176[a]	9.72	—	0.26[a]
4	178	—	176[a]	12.6	—	0.43[a]
5	172	156[a]	163[a]	11.6	0.24[a]	0.30[a]
6	168	—	165[a]*	14.9	—	1.49[a]*
7	164	—	168*	10.0	—	1.33*
8	160	—	171*	12.9	—	2.34*
9	157	—	171*	15.5	—	3.12*

[a] Values extracted from DSC cooling traces.

transition. The values of $\Delta S_{SmAI}/R$ for $m \geq 6$ homologues are several times larger than the values of $\Delta S_{NI}/R$ for $m \leq 5$ as would be expected. The smectic A assignment was also confirmed using X-Ray diffraction for 9O.O5O.O9, Fig. 5. The presented 2D XRD pattern could be interpreted as coming from a tilted smectic phase because the maximum of the diffused high-angle signal is not at an equatorial position with respect to the azimuthal positions of the low-angle diffraction signals. However, in this case it is just an artifact caused by the construction of the heating stage artificially shifting the azimuthal position of the high angle signal. The diffraction pattern of the smectic A phase contained a sharp peak in the small angle region corresponding to a periodicity of 49.50 Å, indicative of a lamellar structure and consistent with the molecular length, suggesting a monolayer packing arrangement. The signal in the wide-angle region was diffuse, indicating a liquid-like ordering within the layers. On cooling there was a negative thermal expansion of the layer spacing (d) and this is typical phase behaviour for an orthogonal smectic phase, Table 2.

The transitional properties for the mO.O6O.Om series are listed in Table 3. The transition temperatures for $m = 2$ were found to be in good agreement with those reported elsewhere.[63] This series also showed N and SmA phases and these were assigned as described earlier, with representative textures shown in Fig. 6. These assignments are supported by the values of $\Delta S_{NI}/R$ which are typical for even-membered dimers[64,65] and

Fig. 5 2D X-ray diffraction pattern for 9O.O5O.O9 in the smectic A phase (T = 150 °C).

**Table 2** The dependence of the layer spacing (d) on temperature for 9O.O5O.O9 measured on cooling

Temperature/°C	d/Å
165	49.50
160	49.70
155	49.90
150	50.05

Table 3 Transition temperatures and associated scaled entropy changes for the mO.O6O.Om series

m	T_{Cr-}/°C	T_{SmAN}/°C	T_{NI}/°C T_{SmAI}*/°C	ΔS_{Cr-}/R	ΔS_{SmAN}/R	ΔS_{NI}/R ΔS_{SmAI}/R*
1	216	—	235	20.3	—	1.74
2	205	—	241	19.4	—	2.12
3	209	—	220	20.9	—	1.76
4	202	—	218	20.1	—	1.98
5	196	199[a]	205	20.5	0.37[a]	1.80
6	190	—	205*	20.0	—	3.85*
7	185	—	203*	20.1	—	4.67*
8	181	—	205*	20.4	—	5.24*
9	178	—	203*	20.3	—	5.72*

[a] Values extracted from DSC cooling traces.

much larger than the values seen for the mO.O5O.Om series. The values of $\Delta S_{SmAI}/R$ for $m \geq 6$ homologues are over twice as
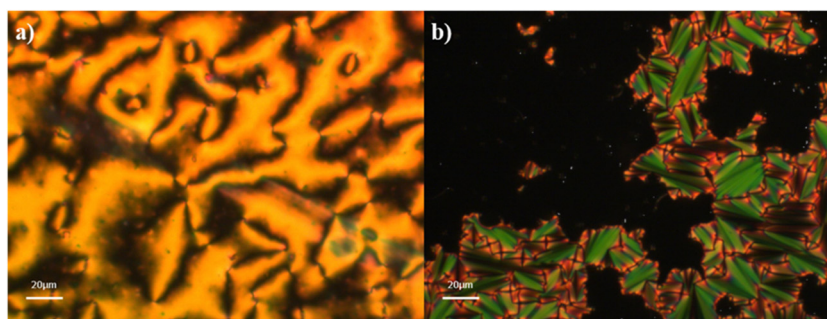
Fig. 4 Textures observed for the mO.O5O.Om series: (a) schlieren texture of the nematic phase (T = 163 °C) for 5O.O5O.O5 and (b) focal conic fan texture with homeotropic regions of the smectic A phase (T = 165 °C) for 9O.O5O.O9.
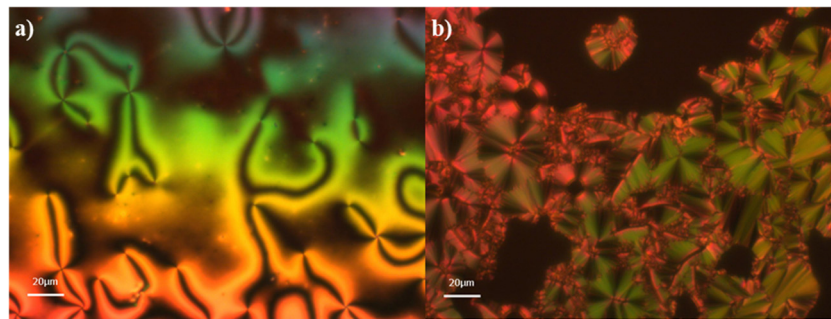
Fig. 6 Textures observed for the mO.O6O.Om series: (a) schlieren texture of the nematic phase (T = 215 °C) for 1O.O6O.O1 and (b) focal conic fan texture with homeotropic regions of the smectic A phase (T = 205 °C) for 8O.O6O.O8.

large as the values of $\Delta S_{NI}/R$ for $m \leq 5$, and also twice as large as the values of $\Delta S_{SmAI}/R$ for the mO.O5O.Om series.

Fig. 7 shows the dependence of the transition temperatures of the mO.O5O.Om series and the mO.O6O.Om series on the length of the terminal chains, m. The values of T_{NI} for both

series show an odd–even effect as m increases in which the even members show the higher values, and the trend in T_{NI} for both the odd and even values of m is decreasing. The alternation is associated with the change in shape on varying the parity of m and has been discussed in detail elsewhere.[57,65–69] The
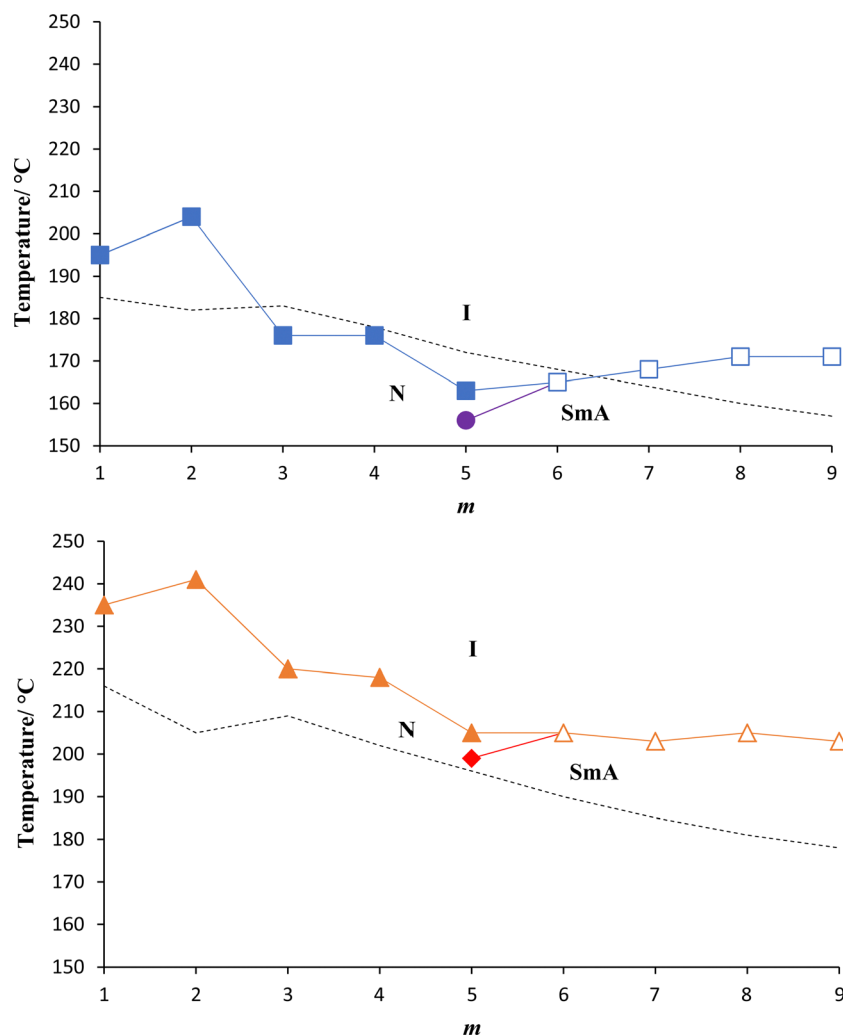

Fig. 7 The dependence of the transition temperatures on m. The mO.O5O.Om series (top) represented by filled squares for T_{NI}, open squares for T_{SmAI} and the filled circle for T_{SmAN}. The mO.O6O.Om series (bottom) represented by filled triangles for T_{NI}, open triangles for T_{SmAI} and the filled diamond for T_{SmAN}. The dotted lines indicate the melting points.

decreasing trend apparent in T_{NI} reflects the increased mole fraction of the alkyloxy chains and this dilutes the interactions between the mesogenic units.[57,70,71] The SmA phase appears at $m = 5$ in both series and the nematic behaviour is extinguished at $m = 6$. This behaviour is consistent with the empirical relationship established for the $m.OnO.m$ family by Date el $al.$[57]

The dependence of the transition temperatures on m for the two series is clearly very similar, but the clearing temperatures for the mO.O6O.Om series are around 40 °C higher than those of the mO.O5O.Om series. This reflects the difference in shape between even- and odd-membered dimers described earlier and shown in Fig. 8. The more bent structure of the odd-membered dimers is less compatible with the nematic environment and so lower T_{NI} values are observed. The higher values of T_{SmAI} seen for the mO.O6O.Om series strongly suggest that the more linear shapes of the even member dimers are able to pack more efficiently into layered structures.

The transitional properties for the mS.O5O.Sm series are listed in Table 4. The homologues with an alkylthio chain with $m \leq 4$ showed a conventional monotropic nematic phase, N. The nematic phase was again assigned by the observation of characteristic schlieren textures as was described earlier and shown in Fig. 9. The value of $\Delta S_{NI}/R$ for 1S.O5O.S1 is consistent with this assignment although it is rather low.[64,65] For $m \geq 5$ no liquid crystalline behaviour was observed, and this was presumably precluded by crystallisation.

The dependence of the nematic–isotropic transition temperatures on the length of the terminal alkylthio chain, m, for the mS.O5O.Sm series is shown in Fig. 10. The nematic behaviour seen for the mS.O5O.Sm series is monotropic in nature and the highest value of T_{NI} is observed for 1S.O5O.S1. As the terminal chain length increases, there is a rapid fall in T_{NI} until $m = 3$ for which a minimum value of T_{NI} is reached and on increasing m further to $m = 4$, T_{NI} increases. The absence of mesogenic behaviour beyond $m = 4$ is most likely due to the very monotropic nature of the nematic phase and crystallisation precludes the observation of liquid crystalline behaviour. Fig. 10 also shows the clearing temperatures of the mO.O5O.Om and m.O5O.m series.[57] In comparing these series it is important to compare homologues which have the same total terminal chain length, t. Heteroatoms incorporated into the terminal chain, such as the sulfur or oxygen linking group, are included in the total length such that $t = m + 1$ for the mS.O5O.Sm and mO.O5O.Om series, whereas $t = m$ for the m.O5O.m series.[57]

The mO.O5O.Om series shows the highest values of both T_{NI} and T_{SmAI} across all terminal chain lengths. Both the mO.O5O.Om and m.O5O.m series show a clear alternation in the values of T_{NI} according to the parity of the total terminal

Table 4 Transition temperatures and associated scaled entropy changes for the mS.O5O.Sm series

m	T_{CrI}/°C	T_{NI}/°C	$\Delta S_{CrI}/R$	$\Delta S_{NI}/R$
1	165	158[a]	12.7	0.19[a]
2	150	121[b]	14.8	—
3	119	84[b]	16.1	—
4	122	95[b]	15.5	—
5	124	—	16.4	—
6	126	—	16.2	—
7	122	—	16.0	—
8	120	—	17.5	—
9	121	—	16.7	—

[a] Values extracted from DSC cooling traces. [b] Measured using the polarised light microscope.

chain length as described earlier. The mS.O5O.Sm series shows values of T_{NI} that are considerably lower than those for the two other series for $t = 3$ to $t = 5$. However, for $t = 2$, 1S.O5O.S1 shows a higher value of T_{NI} than 2.O5O.2 by 32 °C. The value of T_{NI} for 1S.O5O.S1 is 37 °C below that of 1O.O5O.O1. By comparison, for $t = 4$, 3S.O5O.S4 has a T_{NI} which is 38 °C below that of 4.O5O.4 and 92 °C lower than that of 3O.O5O.O3. The higher values of T_{NI} seen for the mO.O5O.Om series may be attributed to the molecular shapes of the compounds having the same length of terminal chains, Fig. 11. 2O.O5O.O2 has the largest bond angle connecting the mesogenic unit and the alkyloxy chain, $i.e.$ C–O–C, and hence is the most linear of the three compounds. The C–O–C bond angle was calculated by DFT to be 119°. The 2S.O5O.S2 dimer is the least linear, with a C–S–C bond angle of 100.5° and this is smaller than the C–C–C bond angle of 113.5° in 3.O5O.3, see Fig. 11. The more acute C–S–C bond angle means that the terminal chain protrudes at more of an angle which reduces the shape anisotropy to a greater extent. It should be noted that the ether-linked terminal chain lies in the plane of the ring to which it is attached, further enhancing structural shape anisotropy. It is clear, however that, the homologues with the shortest terminal chain lengths in the mS.O5O.Sm series show anomalously high values of T_{NI} and similar behaviour has been reported for other materials.[5,11,32,58] This will be discussed in greater detail later.

The transitional properties for the mS.O6O.Sm series are listed in Table 5. The members of the mS.O6O.Sm series with $m \leq 7$ showed a conventional nematic phase, N, and a representative schlieren texture is shown in Fig. 12(a). This assignment is supported by the values of $\Delta S_{NI}/R$ which are typical for even-membered dimers.[64,65] These values are smaller than those of the mO.O6O.Om series which may be accounted for by the enhanced molecular biaxiality arising from the inclusion of the sulfur atom.[47] For the homologues
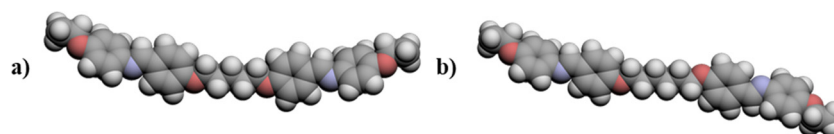

Fig. 8 Space-filling models comparing the molecular shapes of (a) 2O.O5O.O2 and (b) 2O.O6O.O2.
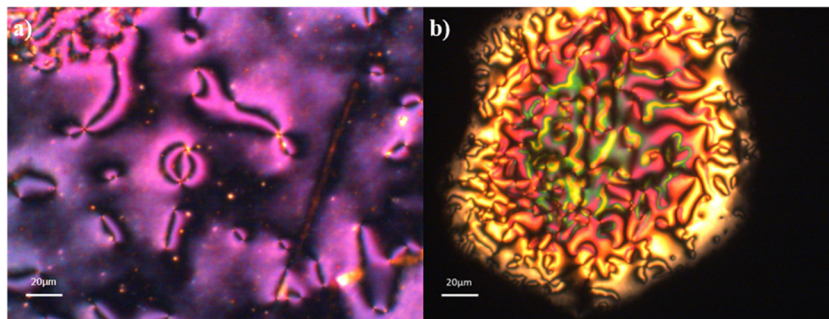
Fig. 9 Textures observed for the mS.O5O.Sm series: (a) schlieren texture of the nematic phase (T = 157 °C) for 1S.O5O.S1 and (b) schlieren texture of the nematic phase (T = 118 °C) for 2S.O5O.S2.
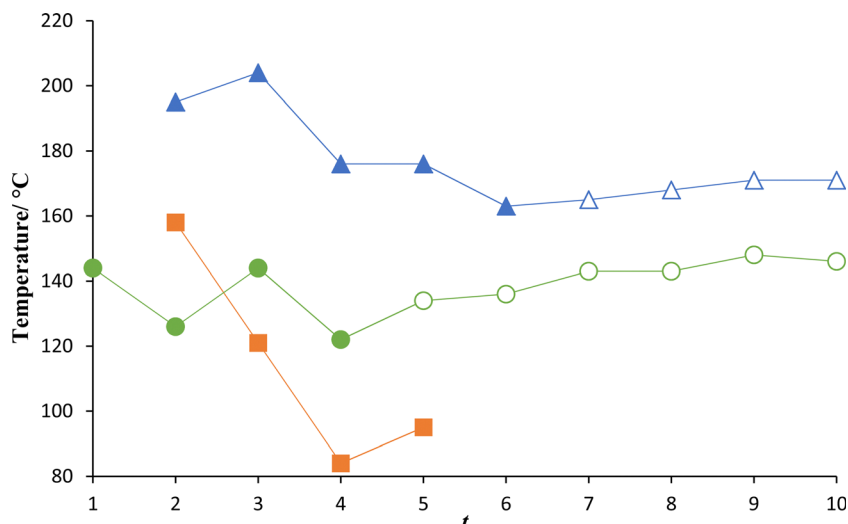

Fig. 10 Comparison of the clearing temperatures for the mS.O5O.Sm series (squares), m.O5O.m series (circles) and mO.O5O.Om series (triangles). The filled symbols denote T_{NI} and the open symbols T_{SmAI}. The temperatures are plotted as a function of the total terminal chain length, t, such that $t = m + 1$ for the mS.O5O.Sm and mO.O5O.Om series, whereas $t = m$ for the m.O5O.m series. The melting points are omitted for clarity.
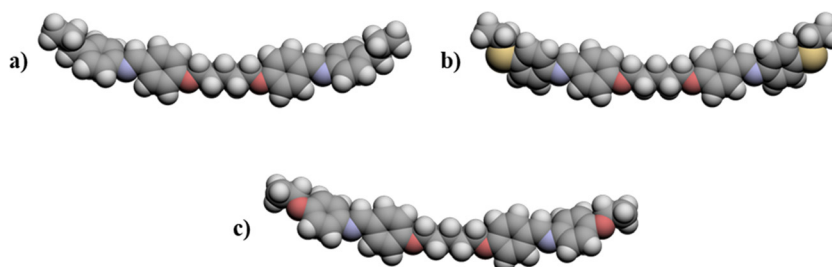

Fig. 11 A comparison of the molecular shapes of (a) 3.O5O.3; (b) 2S.O5O.S2 and (c) 2O.O5O.O2.

with $m \geq 8$, a focal conic fan texture formed directly from the isotropic liquid phase which could be sheared to give a schlieren texture, Fig. 12(b), characteristic of a smectic C phase. The values of $\Delta S_{SmCI}/R$ for the $m \geq 8$ homologues are much larger than the values of $\Delta S_{NI}/R$ for $m \leq 7$. The diffraction pattern of the smectic C phase shown by 9S.O6O.S9 contained a series of sharp commensurate peaks in the small angle region,

indicative of a lamellar structure and corresponding to a periodicity of 47.7 Å, slightly smaller than the molecular length of 50.3 Å. The signal in the wide-angle region was diffuse, indicating a liquid-like ordering within the layers, Fig. 13. On cooling, the layer spacing (d) decreased and this is typical behaviour for a tilted smectic phase supporting the assignment of the smectic C phase, Fig. 14. Upon further cooling, the

Table 5 Transition temperatures and associated scaled entropy changes for the mS.O6O.Sm series

m	$T_{Cr-}/°C$	$T_{SmCI}/°C$	$T_{NI}/°C$	$\Delta S_{Cr-}/R$	$\Delta S_{SmCI}/R$	$\Delta S_{NI}/R$
1	198	—	211	14.2	—	1.78
2	184	—	181[a]	16.8	—	1.41[a]
3	157	—	152[a]	14.8	—	0.88[a]
4	178	—	158[a]	19.9	—	0.97[a]
5	157	—	149[b]	20.2	—	—
6	156	—	150[b]	20.8	—	—
7	153	—	148[b]	20.5	—	—
8	151	154	—	24.8	4.95	—
9	149	153	—	18.7	5.67	—

[a] Values extracted from DSC cooling traces. [b] Measured using the polarised light microscope.

Fig. 13 2D X-ray diffraction pattern for 9S.O6O.S9 in the smectic C phase ($T = 148$ °C).

sample crystallises but there does appear to be a clear crystal-crystal transition with the higher temperature crystal showing a long periodicity (modulation) along the layers.

The dependence of the transition temperatures on the length of the terminal alkyl chain, m, for the mS.O6O.Sm series is shown in Fig. 15 and this behaviour is very similar to that seen for the mS.O5O.Sm series shown in Fig. 10. The highest value of T_{NI} is observed when $m = 1$ and as the terminal chain increases in length, T_{NI} decreases rapidly until $m = 3$, where the trend changes. On increasing m beyond $m = 3$, T_{NI} increases, and a small alternation is observed in which the even homologues show the higher values of T_{NI}. Smectic C phase behaviour emerges at $m = 8$. Fig. 15 also shows the clearing temperatures of the mO.O6O.Om and m.O6O.m series,[57] and as before this comparison is made on the basis of total terminal chain length. The mO.O6O.Om series shows the highest clearing temperatures regardless of the terminal chain length. Both the mO.O6O.Om and m.O6O.m series show a clear alternation in the values of T_{NI} according to the parity of the total terminal chain. This is similar to the behaviour seen for the mO.O5O.m and m.O5O.m series in Fig. 10 and may be accounted for similarly. Again, the behaviour of the dimers containing thioether-linked chains is very different for the shortest members. For $t = 2$, 1S.O6O.S1 has a clearing temperature 25 °C above that of 2.O6O.2 and 24 °C below that of 1O.O6O.O1. When the terminal chain is extended to $t = 4$, 3S.O6O.S3 has a clearing temperature 30 °C below that of 4.O6O.4 and 68 °C below that of 3O.O6O.O3. It is interesting to note that for the
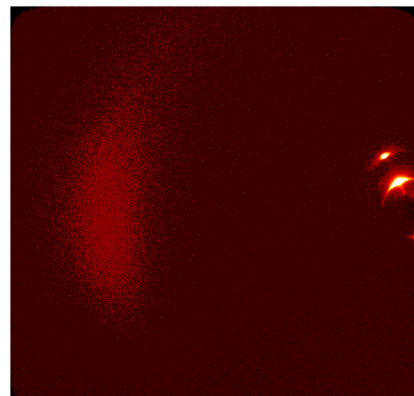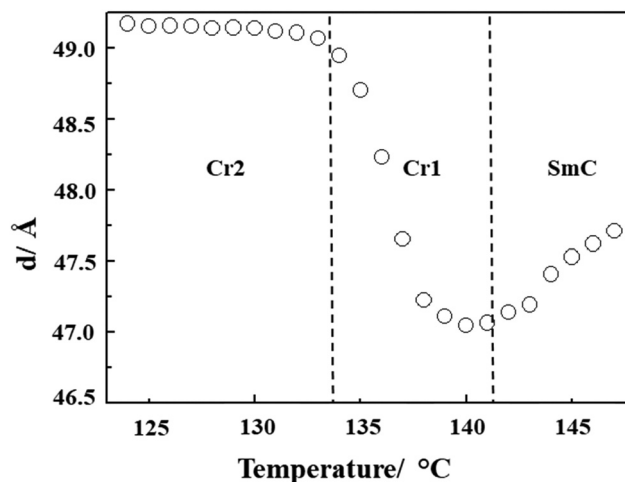

Fig. 14 The dependence of the layer spacing (d) on temperature for 9S.O6O.S9 measured on cooling.

mS.O6O.Sm series, smectic phase behaviour is first observed for $m = 8$, whereas for the mO.O6O.Om and m.O6O.m series, smectic phase behaviour is seen for shorter terminal chains, $m = 5$ and 4, respectively. This is an inversion of the behaviour seen for the nSCB series,[5] specifically when compared to the nOCB and nCB series, the nSCB series was the first to display smectogenic behaviour as n was increased. The switch from

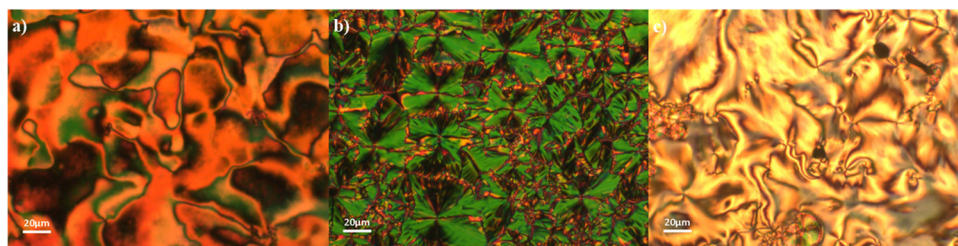**Fig. 12** Textures observed for the mS.O6O.Sm series: (a) schlieren texture of the nematic phase ($T = 208$ °C) for 1S.O6O.S1; (b) focal conic fan texture in a planar aligned cell of the smectic C phase ($T = 151$ °C) for 9S.O6O.S9 and (c) sheared region in untreated glass slides showing the schlieren texture of the smectic C phase ($T = 151$ °C) for 9S.O6O.S9.
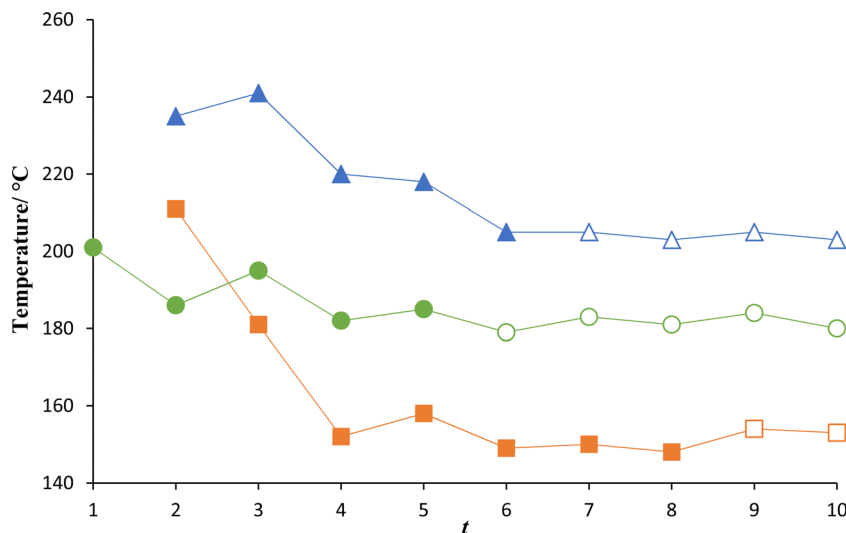
Fig. 15 Comparison of clearing temperatures for the mS.O6O.Sm series (squares), the m.O6O.m series (circles) and the mO.O6O.Om series (triangles); filled symbols denoting T_{NI} and open symbols T_{SmAI} or T_{SmCI}. The temperatures are plotted as a function of the total terminal chain, t, such that $t = m + 1$ for the mS.O6O.Sm and mO.O6O.Om series, whereas $t = m$ for the m.O6O.m series. The melting points are omitted for clarity.

SmA–I transitions seen for the m.O6O.m[57] and mO.O6O.Om series, to SmC–I transitions for the mS.O6O.Sm series may reflect the larger sulfur atom and the lower rotational barrier around the S–C bond. The larger volume occupied by the alkylthio chain compared to the alkyloxy and alkyl terminal chains will fill space more effectively in a tilted phase[72] and a similar effect is observed on branching a terminal chain in non-symmetric dimers.[73]

We now return to the anomalous behaviour seen for the dependence of T_{NI} on m in both the mS.O6O.Sm and mS.O5O.Sm series, with similar behaviour seen for the nSCB series.[5] The rapid decrease in T_{NI} over the first three members of these series was also seen for the non-symmetric dimeric series, CB6O.Sm.[58] This behaviour has been accounted for in terms of chalcogen bonding with regards to the nSCB series.[5] However, other low molar mass mesogens with alkylthio chains have been reported to show similarly anomalous transition temperatures, and these were attributed to the larger dispersion force of the polarisable sulfur when compared to oxygen and carbon.[11,32] Fig. 16 compares the electrostatic potential surfaces of 3S.O5O.S3 to 4.O5O.4 and 3O.O5O.O3. Earlier we accounted for the differences in the transition temperatures of

these series in terms of their average molecular shapes, but these surfaces reveal they also differ in terms of their electron distribution. It is apparent that the increased polar and polarisable nature of the oxygen and sulfur atoms compared to the methylene group changes the electronic distribution associated with the terminal phenyl ring. This will lead to enhanced dipolar interactions promoting both the melting and clearing temperatures compared to the m.O5O.m series. The differences between 3S.O5O.S3 and 3O.O5O.O3 electronically are less apparent and presumably indicate that, as we suggested earlier, the differences in their transitional properties are more linked to the change in shape arising from interchanging the oxygen and sulfur atoms in the terminal chains.

For the CB6O.Sm series, single crystal diffraction studies revealed there was no direct S–S contacts in the crystalline state.[58] Arakawa et al also reported single crystal diffraction studies for a set of low molar mass materials with alkylthio terminal chains that indicated a specific interaction between the sulfur atoms was unlikely to be significant.[11] Such crystal studies, however, cannot completely exclude the possibility that within mesophases such interactions occur. A recent comparison study also reports anomalously high values of T_{NI} for the
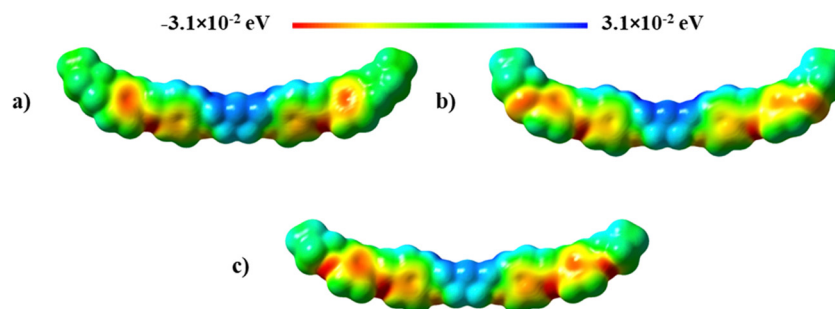

Fig. 16 A comparison of the electrostatic potential surfaces of (a) 4.O5O.4; (b) 3S.O5O.S3 and (c) 3O.O5O.O3.

shortest members of the alkylthio-based series and the authors attribute this to spatially averaged dispersion forces[32] rather than chalcogen bonding.[5] On increasing the terminal chain length, these enhanced dispersion forces are diluted and hence T_{NI} falls, whereas in the crystal phase, microphase separation reinforces these interactions and T_m is seen generally to increase. These dispersion forces were also used to justify the behaviour observed for the nSeCB series.[74] In the dimers we report here, it is not clear why the small structural change passing from 1S.O6O.S1 to 3S.O6O.S3 has such a large effect on T_{NI}, falling by 59 °C. In order to fully understand the trends seen for T_{NI}, further study is required.

Conclusions

Here we have reported how changing the nature of the links between the terminal chains and mesogenic units effects the phase behaviour of symmetric liquid crystal dimers. For short terminal chains, all six series exhibit the nematic phase. On increasing the chain length, smectic phase behaviour is observed for all but the mS.O5O.Sm series. This behaviour is consistent with the empirical relationship established for the m.OnO.m family by Date *el al*.[57] The dimers containing alkyloxy terminal chains showed the highest clearing temperatures, and the sulfur linked dimers the lowest. Anomalously high values of T_{NI}, however, are seen for 2S.O5O.S2 and 2S.O6O.S2. This observation is similar to that observed for the nSCB series[5] and CB6O.Sm series.[58] This has been attributed elsewhere to the larger dispersion force of the polarisable sulfur when compared to oxygen and carbon.[11,32] Further work now needs to be performed to establish and understand the extent to which steric and electronic factors drive the anomalous phase behaviour that appears to be rather general in low molar mass mesogens containing short terminal alkylthio chains.

Conflicts of interest

There are no conflicts of interest to declare.

Acknowledgements

References

1 B. Kohne, K. Praefcke and G. Heppke, Liquid Crystalline 4'-Pentylphenyl 4-Alkyloxydithiobenzoates, *Isr. J. Chem.*, 1979, **18**, 197–198.

2 H. Zaschke, A. Isenberg and H. Schubert, Der kristallinflüssige Zustand als Kriterium zur Konstitutionsermittlung von Derivaten tautomeriefähiger heterocyclischer Systeme. I. Kristallin-flüssige Benzoesäure- und Thiobenzoesäurepyrimidinyl-(2)-ester, *J. Prakt. Chem.*, 1979, **321**, 619–628.

3 W. Elser, The Mesomorphic Behavior of Sulfur Containing Steroid Derivatives, *Mol. Cryst.*, 1969, **8**, 219–232.

4 J. A. Castellano, M. J. E. Goldmacher, L. A. Barton and J. S. Kane, Liquid Crystals. II. Effects of Terminal Group Substitution on the Mesomorphic Behavior of Some Benzylideneanilines, *J. Org. Chem.*, 1968, **33**, 3501–3504.

5 E. Cruickshank, G. J. Strachan, J. M. Storey and C. T. Imrie, Chalcogen bonding and liquid crystallinity: Understanding the anomalous behaviour of the 4'-(alkylthio)[1,1'-biphenyl]-4-carbonitriles (*n*SCB), *J. Mol. Liq.*, 2021, **346**, 117094.

6 Y. Arakawa, S. Inui and H. Tsuji, Synthesis, phase transitions, and liquid crystal behavior of alkylthio azobenzenes, *Tetrahedron*, 2022, **122**, 132958.

7 Y. Arakawa, S. Inui, K. Igawa and H. Tsuji, Alkylthio- and alkyl-substituted asymmetric diphenyldiacetylene-based liquid crystals: phase transitions, mesophase and single-crystal structures, and birefringence, *Liq. Cryst.*, 2019, **46**, 1621–1630.

8 Y. Arakawa, Y. Sasaki and H. Tsuji, Supramolecular hydrogen-bonded liquid crystals based on 4-n-alkylthiobenzoic acids and 4,4'-bipyridine: Their mesomorphic behavior with comparative study including alkyl and alkoxy counterparts, *J. Mol. Liq.*, 2019, **280**, 153–159.

9 Y. Arakawa, S. Kang, H. Tsuji, J. Watanabe and G. I. Konishi, Development of novel bistolane-based liquid crystalline molecules with an alkylsulfanyl group for highly birefringent materials, *RSC Adv.*, 2016, **6**, 16568–16574.

10 Y. Arakawa, Y. Sasaki, N. Haraguchi, S. Itsuno and H. Tsuji, Synthesis, phase transitions and birefringence of novel liquid crystalline 1,4-phenylene bis(4-alkylthio benzoates) and insights into the cybotactic nematic behaviour, *Liq. Cryst.*, 2018, **45**, 821–830.

11 Y. Arakawa, Y. Ishida, Y. Sasaki, S. Sasaki, M. Tokita and H. Tsuji, Alkylthio-based asymmetric liquid crystals: unravelling the substituent effects and intercalated cybotactic nematic and smectic phases, *Mater. Adv.*, 2022, **3**, 3218–3228.

12 M. Alaasar, A. F. Darweesh, X. Cai, F. Liu and C. Tschierske, Mirror Symmetry Breaking and Network Formation in Achiral Polycatenars with Thioether Tail, *Chem. – Eur. J.*, 2021, **27**, 14921–14930.

13 Y. Arakawa, Y. Sasaki, K. Igawa and H. Tsuji, Hydrogen bonding liquid crystalline benzoic acids with alkylthio groups: phase transition behavior and insights into the cybotactic nematic phase, *New J. Chem.*, 2017, **41**, 6514–6522.

14 Y. Arakawa, S. Kang, J. Watanabe and G. I. Konishi, Assembly of thioether-containing rod-like liquid crystalline materials assisted by hydrogen-bonding terminal carboxyl groups, *RSC Adv.*, 2015, **5**, 8056–8062.

15 A. J. Seed, K. J. Toyne and J. W. Goodby, Synthesis of some 2,4- and 2,5-disubstituted thiophene systems and the effect of the pattern of substitution on the refractive indices, optical anisotropies, polarisabilities and order parameters in comparison with those of the parent biphenyl and dithien, *J. Mater. Chem.*, 1995, **5**, 653–661.

16 A. Seed, Synthesis of self-organizing mesogenic materials containing a sulfur-based five-membered heterocyclic core, *Chem. Soc. Rev.*, 2007, **36**, 2046–2069.

17 M. K. Reddy, K. S. Reddy, M. Prakash and T. Narasimhaswamy, Synthesis and Characterization of Two Phenyl Ring Core-Based Thiophene Mesogens, *Mol. Cryst. Liq. Cryst.*, 2013, **582**, 1–14.

18 Y. Arakawa, S. Kang, S. Nakajima, K. Sakajiri, S. Kawauchi, J. Watanabe and G. Konishi, Synthesis of new wide nematic diaryl-diacetylenes containing thiophene-based heteromonocyclic and heterobicyclic structures, and their birefringence properties, *Liq. Cryst.*, 2014, **41**, 642–651.

19 M. Hird, A. J. Seed, K. J. Toyne, J. W. Goodby, G. W. Gray and D. G. McDonnell, Synthesis, transition temperatures and optical anisotropy of some isothiocyanato-substituted biphenyls, *J. Mater. Chem.*, 1993, **3**, 851–859.

20 G. J. Cross, A. J. Seed, K. J. Toyne, J. W. Goodby, M. Hird and M. C. Artal, Synthesis, transition temperatures, and optical properties of compounds with simple phenyl units linked by double bond, triple bond, ester or propiolate linkages, *J. Mater. Chem.*, 2000, **10**, 1555–1563.

21 A. J. Seed, K. J. Toyne, J. W. Goodby and D. G. McDonnell, Synthesis, optical anisotropies, polarisabilities and order parameters of 4-cyanophenyl and 4-isothiocyanatophenyl 4′-butylsulfanylbenzoates with oxygen and sulfur substitution in the ester linkage, *J. Mater. Chem.*, 1995, **5**, 1–11.

22 Z. Fang and C. Wu, Investigation on thermal behaviour and optical properties of non-symmetric cholesterol-based twin liquid crystals with thioester linkages, *Liq. Cryst.*, 2020, **47**, 1086–1099.

23 Y. Arakawa and H. Tsuji, Phase transitions and birefringence of bistolane-based nematic molecules with an alkyl, alkoxy and alkylthio group, *Mol. Cryst. Liq. Cryst.*, 2017, **647**, 422–429.

24 G. W. Gray and S. M. Kelly, Liquid crystals for twisted nematic display devices, *J. Mater. Chem.*, 1999, **9**, 2037–2050.

25 P. Kirsch and M. Bremer, Nematic Liquid Crystals for Active Matrix Displays: Molecular Design and Synthesis, *Angew. Chem., Int. Ed.*, 2000, **39**, 4216–4235.

26 H. R. Stapert, S. Del Valle, E. J. K. Verstegen, B. M. I. Van der Zande, J. Lub and S. Stallinga, Photoreplicated Anisotropic Liquid-Crystalline Lenses for Aberration Control and Dual-Layer Readout of Optical Discs, *Adv. Funct. Mater.*, 2003, **13**, 732–738.

27 P. Valley, G. Peyman, N. Peyghambarian, D. L. Mathine, M. R. Dodge and J. Schwiegerling, Tunable-focus flat liquid-crystal diffractive lens, *Opt. Lett.*, 2010, **35**, 336–338.

28 N. Bennis, T. Jankowski, O. Strzezysz, A. Pakua, D. C. Zografopoulos, P. Perkowski, J. M. Sánchez-Pena, J. M. López-Higuera and J. F. Algorri, A high birefringence liquid crystal for lenses with large aperture, *Sci. Rep.*, 2022, **12**, 1–12.

29 M. G. Chee, M. H. Song, D. Kim, H. Takezoe and I. J. Chung, Lowring Lasing Threshold in Chiral Nematic Liquid Crystal Structure with Different Anisotropies, *Jpn. J. Appl. Phys.*, 2007, **46**, L437.

30 L. Driencourt, F. Federspiel, D. Kazazis, L. T. Tseng, R. Frantz, Y. Ekinci, R. Ferrini and B. Gallinet, Electrically Tunable Multicolored Filter Using Birefringent Plasmonic Resonators and Liquid Crystals, *ACS Photonics*, 2020, **7**, 444–453.

31 D. Franklin, Y. Chen, A. Vazquez-Guardado, S. Modak, J. Boroumand, D. Xu, S. T. Wu and D. Chanda, Polarization-independent actively tunable colour generation on imprinted plasmonic surfaces, *Nat. Commun.*, 2015, **6**, 1–8.

32 Y. Arakawa, Y. Ishida, T. Shiba, K. Igawa, S. Sasaki and H. Tsuji, Effects of alkylthio groups on phase transitions of organic molecules and liquid crystals: a comparative study with alkyl and alkoxy groups, *CrystEngComm*, 2022, **24**, 1877–1890.

33 Y. Arakawa, S. Inui and H. Tsuji, Novel diphenylacetylene-based room-temperature liquid crystalline molecules with alkylthio groups, and investigation of the role for terminal alkyl chains in mesogenic incidence and tendency, *Liq. Cryst.*, 2018, **45**, 811–820.

34 C. T. Imrie and P. A. Henderson, Liquid crystal dimers and higher oligomers: Between monomers and polymers, *Chem. Soc. Rev.*, 2007, **36**, 2096–2124.

35 C. T. Imrie, P. A. Henderson and G. Y. Yeap, Liquid crystal oligomers: Going beyond dimers, *Liq. Cryst.*, 2009, **36**, 755–777.

36 M. Cestari, S. Diez-Berart, D. A. Dunmur, A. Ferrarini, M. R. De La Fuente, D. J. B. Jackson, D. O. Lopez, G. R. Luckhurst, M. A. Perez-Jubindo, R. M. Richardson, J. Salud, B. A. Timimi and H. Zimmermann, Phase behavior and properties of the liquid-crystal dimer 1″,7″-bis(4-cyanobiphenyl-4′-yl) heptane: A twist-bend nematic liquid crystal, *Phys. Rev. E: Stat., Nonlinear, Soft Matter Phys.*, 2011, **84**, 031704.

37 R. J. Mandle, A Ten-Year Perspective on Twist-Bend Nematic Materials, *Molecules*, 2022, **27**, 2689.

38 V. Borshch, Y. K. Kim, J. Xiang, M. Gao, A. Jákli, V. P. Panov, J. K. Vij, C. T. Imrie, M. G. Tamba, G. H. Mehl and O. D. Lavrentovich, Nematic twist-bend phase with nano-scale modulation of molecular orientation, *Nat. Commun.*, 2013, **4**, 2635.

39 D. Chen, J. H. Porada, J. B. Hooper, A. Klittnick, Y. Shen, M. R. Tuchband, E. Korbloèa, D. Bedrov, D. M. Walba, M. A. Glaser, J. E. Maclennan and N. A. Clark, Chiral heliconical ground state of nanoscale pitch in a nematic liquid crystal of achiral molecular dimers, *Proc. Natl. Acad. Sci. U. S. A.*, 2013, **110**, 15931–15936.

40 J. P. Abberley, R. Killah, R. Walker, J. M. D. Storey, C. T. Imrie, M. Salamończyk, C. Zhu, E. Gorecka and D. Pociecha, Heliconical smectic phases formed by achiral molecules, *Nat. Commun.*, 2018, **9**, 228.

41 C. T. Imrie, R. Walker, J. M. D. D. Storey, E. Gorecka and D. Pociecha, Liquid Crystal Dimers and Smectic Phases from the Intercalated to the Twist-Bend, *Crystals*, 2022, **12**, 1245.

42 M. Salamończyk, N. Vaupotič, D. Pociecha, R. Walker, J. M. D. Storey, C. T. Imrie, C. Wang, C. Zhu and E. Gorecka, Multi-level chirality in liquid crystals formed by achiral molecules, *Nat. Commun.*, 2019, **10**, 1922.

43 C. T. Imrie, Liquid Crystal Dimers, in *Liquid Crystals II*, ed. D. M. P. Mingos, Springer, New York US, 1999, pp. 149–192.

44 H. C. Lee, Z. Lu, P. A. Henderson, M. F. Achard, W. A. K. Mahmood, G. Y. Yeap and C. T. Imrie, Cholesteryl-based liquid crystal dimers containing a sulfur–sulfur link in the flexible spacer, *Liq. Cryst.*, 2012, **39**, 259–268.

45 S. K. Pal, V. A. Raghunathan and S. Kumar, Phase transitions in novel disulphide-bridged alkoxycyanobiphenyl dimers, *Liq. Cryst.*, 2007, **34**, 135–141.

46 P. W. Yap, F. Osman, G. Y. Yeap, Y. Nakamura, K. Kaneko, A. Shimizu and M. M. Ito, Non-linear disulphide-centred S-shaped oligomers with inner and outer spacers connected by aromatic azo moieties, *Liq. Cryst.*, 2022, DOI: 10.1080/02678292.2022.2127161.

47 E. Cruickshank, M. Salamończyk, D. Pociecha, G. J. Strachan, J. M. D. Storey, C. Wang, J. Feng, C. Zhu, E. Gorecka and C. T. Imrie, Sulfur-linked cyanobiphenyl-based liquid crystal dimers and the twist-bend nematic phase, *Liq. Cryst.*, 2019, **46**, 1595–1609.

48 Y. Arakawa, K. Komatsu and H. Tsuji, Twist-bend nematic liquid crystals based on thioether linkage, *New J. Chem.*, 2019, **43**, 6786–6793.

49 Y. Arakawa, K. Komatsu, S. Inui and H. Tsuji, Thioether-linked liquid crystal dimers and trimers: The twist-bend nematic phase, *J. Mol. Struct.*, 2020, **1199**, 126913.

50 Y. Arakawa, Y. Ishida, K. Komatsu, Y. Arai and H. Tsuji, Thioether-linked benzylideneaniline-based twist-bend nematic liquid crystal dimers: Insights into spacer lengths, mesogenic arm structures, and linkage types, *Tetrahedron*, 2021, **95**, 132351.

51 Y. Arakawa, K. Komatsu, T. Shiba and H. Tsuji, Methylene- and thioether-linked cyanobiphenyl liquid crystal dimers CB*n*SCB exhibiting room temperature twist-bend nematic phases and glasses, *Mater. Adv.*, 2021, **2**, 1760–1773.

52 Y. Arakawa, K. Komatsu, Y. Ishida and H. Tsuji, Thioether-linked azobenzene-based liquid crystal dimers exhibiting the twist-bend nematic phase over a wide temperature range, *Liq. Cryst.*, 2021, **48**, 641–652.

53 K. Isoda, T. Ichikawa, K. Kaneko, M. Kondo, T. Sakurai, A. Seki, M. Hara, G. Watanabe, Y. Arakawa, Y. Arai, K. Horita, K. Komatsu and H. Tsuji, Twist-Bend Nematic Phase Behavior of Cyanobiphenyl-Based Dimers with Propane, Ethoxy, and Ethylthio Spacers, *Crystals*, 2022, **12**, 1734.

54 Y. Arakawa, Y. Ishida and H. Tsuji, Ether- and Thioether-Linked Naphthalene-Based Liquid-Crystal Dimers: Influence of Chalcogen Linkage and Mesogenic-Arm Symmetry on the Incidence and Stability of the Twist–Bend Nematic Phase, *Chem. – Eur. J.*, 2020, **26**, 3767–3775.

55 Y. Arakawa, K. Komatsu, J. Feng, C. Zhu and H. Tsuji, Distinct twist-bend nematic phase behaviors associated with the ester-linkage direction of thioether-linked liquid crystal dimers, *Mater. Adv.*, 2021, **2**, 261–272.

56 I. Nishiyama, J. Yamamoto, J. W. Goodby and H. Yokoyama, Effect of introducing thioether linkages on the molecular organization of chiral twin liquid crystals, *Liq. Cryst.*, 2004, **31**, 1495–1502.

57 R. W. Date, C. T. Imrie, G. R. Luckhurst and J. M. Seddon, Smectogenic dimeric liquid crystals: The preparation and properties of the α,ω-bis(4-n-alkylanilinebenzylidine-4′-oxy)alkanes, *Liq. Cryst.*, 1992, **12**, 203–238.

58 E. Cruickshank, K. Anderson, J. M. D. Storey, C. T. Imrie, E. Gorecka, D. Pociecha, A. Makal and M. M. Majewska,

59 X. Zong, Z. Fang and C. Wu, Synthesis and mesomorphic properties of a series of dimers derived from thioether-terminated and cholesteryl, *Liq. Cryst.*, 2018, **45**, 1844–1853.

60 R. Saha, C. Feng, C. Welch, G. H. Mehl, J. Feng, C. Zhu, J. Gleeson, S. Sprunt and A. Jákli, The interplay between spatial and heliconical orientational order in twist-bend nematic materials, *Phys. Chem. Chem. Phys.*, 2021, **23**, 4055–4063.

61 M. J. Frisch, G. W. Trucks, H. B. Schlegel, G. E. Scuseria, M. A. Robb, J. R. Cheeseman, G. Scalmani, V. Barone, B. Mennucci, G. A. Petersson, H. Nakatsuji, M. Caricato, X. Li, H. P. Hratchian, A. F. Izmaylov, J. Bloino, G. Zheng, J. L. Sonnenberg, M. Hada, M. Ehara, K. Toyota, R. Fukuda, J. Hasegawa, M. Ishida, T. Nakajima, Y. Honda, O. Kitao, H. Nakai, T. Vreven, J. A. Montgomery, J. E. Peralta, F. Ogliaro, M. Bearpark, J. J. Heyd, E. Brothers, K. N. Kudin, V. N. Staroverov, R. Kobayashi, J. Normand, K. Raghavachari, A. Rendell, J. C. Burant, S. S. Iyengar, J. Tomasi, M. Cossi, N. Rega, J. M. Millam, M. Klene, J. E. Knox, J. B. Cross, V. Bakken, C. Adamo, J. Jaramillo, R. Gomperts, R. E. Stratmann, O. Yazyev, A. J. Austin, R. Cammi, C. Pomelli, J. W. Ochterski, R. L. Martin, K. Morokuma, V. G. Zakrzewski, G. A. Voth, P. Salvador, J. J. Dannenberg, S. Dapprich, A. D. Daniels, Ö. Farkas, J. B. Foresman, J. V. Ortiz, J. Cioslowski and D. J. Fox, *Gaussian 09, Revision B.01*, Gaussian, Inc., Wallingford CT, 2010.

62 M. Tarini, P. Cignoni and C. Montani, Ambient occlusion and edge cueing to enhance real time molecular visualization, *IEEE Trans. Vis. Comput. Graph.*, 2006, **12**, 1237–1244.

63 J.-I. Jin and J.-H. Park, Thermotropic Compounds with Two Terminal Mesogenic Units and a Central Spacer. 5 1. Homologous Series of Polymethylene-α,ω-Bis (*p*-Oxybenzylidene Aniline), *Mol. Cryst. Liq. Cryst.*, 1984, **110**, 293–308.

64 P. J. Barnes, S. K. Heeks, S. K. Heeks and G. R. Luckhurst, An enhanced odd-even effect of liquid crystal dimers Orientational order in the α,ω-bis(4′-cyanobiphenyl-4-yl)alkanes, *Liq. Cryst.*, 2006, **13**, 603–613.

65 P. A. Henderson, O. Niemeyer and C. T. Imrie, Methylene-linked liquid crystal dimers, *Liq. Cryst.*, 2001, **28**, 463–472.

66 C. T. Imrie and L. Taylor, The preparation and properties of low molar mass liquid crystals possessing lateral alkyl chains, *Liq. Cryst.*, 1989, **6**, 1–10.

67 E. Forsyth, D. A. Paterson, E. Cruickshank, G. J. Strachan, E. Gorecka, R. Walker, J. M. D. Storey and C. T. Imrie, Liquid crystal dimers and the twist-bend nematic phase: On the role of spacers and terminal alkyl chains, *J. Mol. Liq.*, 2020, **320**, 114391.

68 R. Walker, D. Pociecha, G. J. Strachan, J. M. D. Storey, E. Gorecka and C. T. Imrie, Molecular curvature, specific intermolecular interactions and the twist-bend nematic phase: the synthesis and characterisation of the 1-(4-cyanobiphenyl-4′-yl)-6-(4-alkylanilinebenzylidene-4′-oxy)hexanes (CB6O.*m*), *Soft Matter*, 2019, **15**, 3188–3197.

69 J. L. Hogan, C. T. Imrie and G. R. Luckhurst, Asymmetric dimeric liquid crystals The preparation and properties of the

Helical phases assembled from achiral molecules: Twist-bend nematic and helical filamentary B4 phases formed by mesogenic dimers, *J. Mol. Liq.*, 2022, **346**, 118180.

α-(4-cyanobiphenyl-4′-oxy)-ω-(4-*n*-alkylanilinebenzylidene-4′-oxy)hexanes, *Liq. Cryst.*, 1988, **3**, 645–650.

70 R. Walker, D. Pociecha, J. M. D. Storey, E. Gorecka and C. T. Imrie, Remarkable smectic phase behaviour in odd-membered liquid crystal dimers: the CT6O.*m* series, *J. Mater. Chem. C*, 2021, **9**, 5167–5173.

71 G. S. Attard, R. W. Date, C. T. Imrie, G. R. Luckhurst, S. J. Roskilly, J. M. Seddon and L. Taylor, Non-symmetric dimeric liquid crystals The preparation and properties of the α-(4-cyanobiphenyl-4′-yloxy)-ω-(4-*n*-alkylanilinebenzylidene-4′-oxy)alkanes, *Liq. Cryst.*, 1994, **16**, 529–581.

72 J. W. Goodby, R. J. Mandle, E. J. Davis, T. Zhong and S. J. Cowling, What makes a liquid crystal? The effect of free volume on soft matter, *Liq. Cryst.*, 2015, **42**, 593–622.

73 R. Walker, D. Pociecha, C. Faidutti, E. Perkovic, J. M. D. Storey, E. Gorecka and C. T. Imrie, Remarkable stabilisation of the intercalated smectic phases of nonsymmetric dimers by *tert*-butyl groups, *Liq. Cryst.*, 2022, **49**, 969–981.

74 Y. Arakawa, T. Shiba, K. Igawa, S. Sasaki and H. Tsuji, 4′-Alkylseleno-4-cyanobiphenyls, *n*SeCB: synthesis and substituent effects on the phase-transition and liquid crystalline behaviors, *CrystEngComm*, 2022, **24**, 7592–7601.